Molecular dynamics simulations of the diffusion and rotation of Pt nanoclusters supported on graphite

Ji Hoon Ryu, Dong Hwa Seo, Da Hye Kim and Hyuck Mo Lee*

We study the diffusion and rotation of Pt nanoclusters supported on graphite. Using molecular dynamics simulation, we reveal that the supported Pt clusters have two types of bottom layers: a hexagonal lattice and a rectangular lattice. The diffusion rate of the Pt clusters mainly depends on the types of bottom layers. This observation is explained by the periodic lattice matching between the bottom layer and the graphite. In addition to lateral diffusion, we find that the Pt clusters with a rectangular or mixed lattice tend to rotate or wag on the z axis. By using the rotation rates and total movements of all atoms, we show that the rotation of a Pt cluster can be induced by the difference in the diffusion rates for the different types of bottom layers. This outcome is well in accord with our diffusion mechanism.

Introduction

Recently, supported nano-sized materials have attracted great attention due to their potential in many physical and chemical processes.[1] Supported Pt nanoclusters are especially useful in many practical applications, such as nanoelectronics, magnetic devices and catalysts in fuel cells.[2] For better catalyst efficiency, Pt clusters need to be dispersed and should not aggregate on the carbon support to increase durability as well as catalytic activity.[3] Because an interaction between the Pt clusters and the carbon support is induced by a weak van der Waals force, there is a considerable aggregation of Pt clusters over time leading to a decrease in surface area and activity.[4] Hence, a better understanding of the dynamics of Pt clusters on a carbon support should help us improve the overall properties of Pt clusters.

Lately, the dynamic properties of Pt clusters supported on graphite have also been studied experimentally by means of surface imaging techniques such as scanning tunneling microscopy (STM),[5–11] atomic force microscopy,[12–16] and transmission electron microscopy.[17] Clark and Kesmodel,[10] for example, reported that Pt clusters diffused on highly oriented pyrolytic graphite form a more stable and larger cluster. In addition, Bardotti *et al.*[18,19] showed that large Au and Sb clusters with one hundred to a few thousand atoms diffused on graphite at a surprisingly high rate of about 10^{-8} cm² s⁻¹ at room temperature. These rates are comparable to those of single atoms. Despite the use of highly developed experimental techniques, however, the task of gaining a detailed understanding of a cluster's dynamic properties, such as diffusion and aggregation, is difficult because imaging techniques only provide temporal discrete images during diffusion processes.

In contrast, molecular dynamics (MD) simulation is a useful tool for understanding the detailed dynamics of an atomic scale because it deals with the dynamic evolution of a picosecond (ps) time scale. In recent years, many successful theoretical investigations have focused on the diffusion and aggregation of supported clusters as well as adatoms.[17,20–28] Using a MD simulation method, Deltour *et al.*[22] reported that the cluster can diffuse rapidly in the order of 10^{-8} cm² s⁻¹ when the lattice parameters of a cluster are incommensurate with those of a substrate, whereas the cluster is epitaxially locked on the substrate in the order of 10^{-17} cm² s⁻¹ when the lattice parameters of the substrate and cluster are commensurate.[29–31] This outcome is in accordance with the experimental results observed by Bardotti *et al.*[18,19] Another MD simulation for the diffusion and aggregation of Au clusters was performed by Lewis *et al.*[24] They showed that a single cluster and cluster dimers diffuse at a rate which is comparable to that of adatoms. Similar results have also been seen in the case of Pd on magnesium oxide with a MD and kinetic Monte Carlo simulations.[28] In their report, it was revealed that fast mobility of clusters larger than a single atom is essential for bringing the theoretical results into agreement with the outcome of molecular beam epitaxy experiments.[32,33]

Although many theoretical studies have been performed on the dynamic properties of supported clusters, relatively little research has examined the rotational motion (pivotal and wagging) of a cluster itself during the diffusion process. In this work, we study the lateral and rotational motion of Pt clusters supported on graphite. Using the MD simulation method, we first analyze the relation between the diffusion rate and the bottom structure of a Pt cluster. On the basis of this analysis, we propose from a periodic lattice matching point of view an advanced diffusion mechanism of supported clusters with graphite. We also investigate the pivotal rotational motion of Pt clusters on the z axis during their diffusion process. This peculiar motion of Pt clusters is explained by our diffusion mechanism. All of these results show that the cluster with lateral motion tends to move faster and further than the cluster with rotational motion at the same running time. We therefore deduce that the cluster which moves rotationally is

Department of Materials Science and Engineering, KAIST, Gwahangno, 335, Yuseong-gu, 305-701 Daejeon, Korea. E-mail: hmlee@kaist.ac.kr; Fax: +82-42-350-3310; Tel: +82-42-350-3334

This journal is © the Owner Societies 2009

Phys. Chem. Chem. Phys., 2009, **11**, 503–507 | 503

more effective for preventing undesirable aggregation than the cluster which moves laterally.

Computational details

We carried out classical MD simulations in canonical ensemble conditions (NVT) with XMD code.[34] To integrate the equation of motion, which is governed by Newton's second law, we used a velocity rescaling algorithm with a time step (Δt) of 0.0005 ps. The quantum Sutton-Chen (Q_SC) potential[35] was used to describe the interaction between the Pt atoms. Because the interaction between the Pt clusters and graphite is mainly dominated by a weak van der Waals force, we used the 12–6 Lennard-Jones (LJ) potential, where the parameter ε_{Pt-C} is 0.040922 eV and the parameter σ_{Pt-C} is 0.2936 nm.[36] For a carbon–carbon interaction, we also used the LJ potential where, according to Steele's group, ε_{C-C} is 0.002413 eV and σ_{C-C} is 0.34 nm.[37]

All MD simulations were conducted in a slab-structured system (7.368 × 6.381 × 30 nm), where periodic boundary conditions are applied along the graphite layers (of the x axis and y axis). The graphite, which consists of two graphene layers arranged in an AB stack with an interlayer spacing of 0.34 nm, is set to the bottom of the simulation box and the Pt nanoclusters are located on the graphite surface. To reduce the computational load of all the MD simulations, we used a static substrate that fixed the positions of all the carbon atoms. For the initial cluster structure, we prepared various Pt_n clusters (where n = 10, 20, 30, 40, 50, 60, 70, 80, 90, 100, 150, 200, 250, 300 atoms) supported on a graphite surface and optimized the clusters with a simulated annealing procedure. Each cluster was heated to 700 K for 50 ps and then allowed to cool to 600, 500 and 400 K with simulated periods of 50 ps, respectively. Finally, each cluster was equilibrated at 298 K for 2700 ps.

To investigate the dynamic properties of Pt clusters, we calculated the diffusion rate (D) as follows from a 2D square displacement:

$$D = \frac{1}{4\Delta t}\langle|(r(t+s)-r(s))|^2\rangle,$$

where $r(t + s)$ and $r(s)$ are the vector positions of the cluster center of mass or all the Pt atoms in the cluster at times $t + s$ and s. $\langle|r(t + s) - r(s)|^2\rangle$ is the mean-square displacement

(MSD) of each case; the cluster center of mass (MSD_{cm}) or all the Pt atoms in the cluster (MSD_{total}). Three consecutive runs were performed to compute the diffusion rates, and the length of each run was 1 ns for each system. The initial configuration of each run is taken from the final configuration of the previous run. The diffusion rates of the three runs were averaged for a more reliable evaluation of the dynamic properties.

Results and discussion

Overall structure and bottom structure of Pt clusters on graphite

To investigate which factors affect the diffusion of Pt clusters supported on graphite, we analyze the static properties as well as dynamic properties of Pt clusters. Table 1 shows the overall structure of the Pt clusters, the bottom layers that are in contact with the graphite surface, the diffusion rates (D_{cm} and D_{total}) and the rotation rates ($100 \times D_{rotation}$) with various Pt clusters. From above, D_{cm}, D_{total} and $D_{rotation}$ are represented as follows:

$$D_{cm} = \frac{MSD_{cm}}{4\Delta t}$$

$$D_{total} = \frac{MSD_{total}}{4\Delta t}$$

$$D_{rotation} = \frac{D_{total} - D_{cm}}{D_{total}}$$

According to Gu and Balbuena,[23] structures of the Pt clusters that fluctuate between ordered (hcp and/or fcc) and less ordered structures depend on two factors: competition between the Pt–Pt and Pt–C interactions and the total number of atoms in the Pt cluster that determine the formation of an atomic closed shell (CS). Depending on these two factors, the supported Pt clusters can be an ordered structure with a fcc or hcp structure or both, or a less ordered structure with a spherical shell.

Fig. 1 shows from left to right the overall structure and the bottom layers of the ordered (Pt_{150}), mixed (Pt_{80}) and less ordered (Pt_{250}) structure. The configurations of Pt_{30}, Pt_{40}, Pt_{70}, Pt_{90} and Pt_{150} reveal an ordered structure with a fcc or hcp

Table 1 Static and dynamic properties of Pt clusters with cluster size

N	Structure	Bottom layer	$D_{cm}/10^{-5}$ cm² s⁻¹	$D_{total}/10^{-5}$ cm² s⁻¹	$100 \times D_{rotation}$
10	CS	Hexa.	14.5258	20.5987	7.3705
20	CS	Hexa.	14.2064	19.9921	7.2349
30	hcp	Hexa.	17.1964	22.6074	5.9837
40	fcc	Hexa.	15.6103	22.3242	7.5187
50	CS	Mixed	3.1583	4.9033	8.8974
60	CS	Mixed	4.4595	6.5009	7.8505
70	fcc + hcp	Hexa.	14.1758	19.2279	6.5687
80	CS + hcp	Mixed	6.8777	15.4601	13.8783
90	Fcc	Hexa.	23.2213	23.3361	0.1229
100	CS	Mixed	1.0385	1.67908	9.5377
150	hcp + fcc	Hexa.	7.4091	10.4400	7.2579
200	CS	Rect.	0.2961	0.5231	10.8491
250	CS	Rect.	0.4239	0.7325	10.5319
300	CS	Mixed	6.2527	17.6868	16.1620
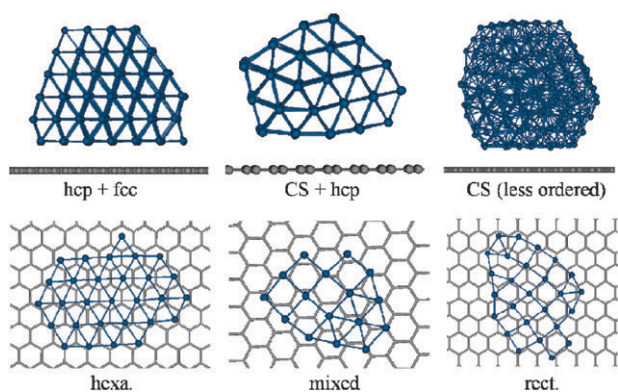
Fig. 1 Overall structures (top row) and bottom layers (bottom row) of the ordered (Pt_{150}), mixed (Pt_{80}) and less ordered (Pt_{250}) structure, from left to right.

Fig. 2 Variation of diffusion rates and bottom layers with cluster size.

structure or both, whereas the remaining clusters except Pt_{80} show a less ordered structure with a spherical shape. Because the Q_SC potential underestimates the hcp-fcc energy difference in the bulk, the hcp structures are highly likely to be found in ordered structures. In the case of Pt_{80}, the overall structure is based on decahedral morphology. This structure was theoretically predicted for this size in the case of free Pt clusters.[38] Although this structure is based on decahedral morphology, the hcp and closed shell structures are also observed simultaneously; hence, we call it a mixed structure in this study.

During the equilibration procedure, an atomic redistribution occurs in the bottom layer of the Pt cluster due to interactions with the graphite surface. At this time, the bottom layers tend to depend on the overall structure of the Pt clusters.[23] In general, ordered structures have a hexagonal lattice with a (111) facet in their bottom layer to match the graphite lattice. On the other hand, the less ordered structures have either a rectangular lattice with a (100) facet or a mixed lattice (where two types of lattices exist simultaneously). These types of bottom lattices have also been reported in many theoretical[20,23,27,36] and experimental studies.[5,6,10] Table 1 also shows the bottom layers in relation to the structure of the Pt clusters. All Pt clusters with an ordered structure have a hexagonal bottom lattice. In contrast, except for the very small clusters (Pt_{10}, Pt_{20}), the Pt clusters with a less ordered or mixed structure have a rectangular or mixed bottom lattice. This result is in accord with other theoretical studies.[20,23]

Dependence of the Pt cluster diffusion rates on the bottom layer

In addition to analyzing the static properties of Pt clusters we also analyzed the dynamic properties. As summarized in Table 1, the calculated values for the diffusion rates of the Pt clusters are somewhere in the order of 10^{-5} cm^2 s^{-1} for D_{cm} and D_{total}. This order of the value is the same as that of other theoretical studies for Pt, Cu, Ni and Au clusters on a graphite surface.[20,24,36,39]

To investigate which factors affect the diffusion rates, we analyzed the interaction between the diffusion rates and the following factors: the overall structure of the Pt clusters, the configuration of the bottom layer, the 1st nearest neighbor,
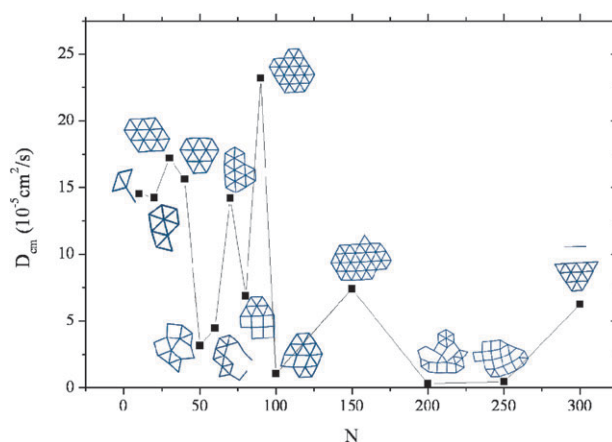
the number of atoms, and the mean bond length in the bottom layer with the size of the Pt cluster. According to Deltour et al.,[22] the diffusion of the cluster depends on the difference in the lattice parameters of the cluster and the substrate. In the Pt–C system, the 1st nearest neighbor and the mean bond length in the bottom layer which represent the lattice parameter of Pt clusters are merely different in the range of 0.01 nm in all Pt clusters. Thus we neglect the effect of the lattice parameters of the cluster and the substrate. Instead, of all these factors, we deduced that the configuration of the bottom layer is the most important factor in relation to the diffusion rate.

Fig. 2 shows the relation between the diffusion rates and the bottom layers of the Pt clusters. All seven peaks for Pt_{10}, Pt_{20}, Pt_{30}, Pt_{40}, Pt_{70}, Pt_{90} and Pt_{150} correspond to the hexagonal bottom layer. As shown in Fig. 2 and Table 1, the diffusion rate depends mainly on the configuration of the bottom layer rather than the cluster size or the overall structure of the Pt cluster. (In Table 1, the 1st nearest neighbor, the number of atoms, and the mean bond length are omitted.) Similar results have been reported in other theoretical[20,21,23] and experimental[12] studies. Lamas and Balbuena[20] confirmed that a Pt cluster on a graphite surface moves rapidly whenever the bottom layer of the cluster is in the shape of a hexagonal lattice but slowly whenever the bottom layer is in the shape of a rectangular or mixed lattice. These results are well accordant with our results.

Generally, the Pt atoms in contact with the graphite surface tend to be arranged with the underlying carbon atoms. Studies based on STM[5,6,10] suggest that the Pt atoms are mostly located at the β sites, the center of the hexagonal ring of the graphite, or at the bridge sites that connect the 1st nearest neighbor of the carbon atoms. When the Pt atoms are mostly located at the β sites of the graphite surface, the bottom layer of the Pt cluster is in the shape of a hexagonal lattice. At the bridge sites, on the other hand, the Pt cluster has a rectangular lattice. According to Lamas and Balbuena,[20] the Pt atoms are constrained to the bridge site because they interact most strongly with the carbon atoms at these positions. Hence, the Pt cluster with the rectangular lattice, the Pt atoms of which are mostly located at the bridge site, cannot move as

easily on the surface as a cluster with a hexagonal lattice. As suggested in the experiment,[6] however, the LJ potential used in our study indicates that Pt atoms interact much stronger at the β site than at the bridge site with carbon atoms. Because of strong interaction at the bridge site, the constraint mechanism referred to in an earlier report[20] cannot properly explain the fast diffusion of a Pt cluster with a hexagonal lattice. Hence, even though the diffusion trends depending on the bottom layer of the cluster are similar to our results, we need different analysis considering strong interaction at the β sites and fast diffusion of a cluster with a hexagonal lattice simultaneously.

To explain this observation, we focus not only on the interaction between the Pt atoms and the carbon atoms but on the periodic lattice matching between the bottom layer of the Pt cluster and the stable sites on the graphite surface. On the graphite surface, the stable β sites are arranged periodically with a hexagonal configuration. Because the Pt atoms in the hexagonal bottom layer have the same periodicity as the β sites of the graphite surface, the Pt cluster can easily find the next stable sites to move to. This capability enables the Pt cluster with the hexagonal lattice to move easily from one stable site to another stable site on the graphite surface. The internal vibration of a cluster can easily overcome the low energy barrier between two stable β sites[5] (about 0.052 eV in our study). In contrast, because a rectangular or a mixed lattice has no periodicity, it has difficulty matching the stable sites on the graphite surface, regardless of whether the sites are β sites or bridge sites. As a result, a Pt cluster with one of those types of bottom layers is unable to find the next stable site to move to and, consequently, cannot diffuse as fast as a Pt cluster with a hexagonal lattice. In this case, the Pt cluster tends to wag or rotate on the z axis rather than move to other stable sites.

Rotation of a Pt cluster during the diffusion process

Aside from observing lateral diffusion during the diffusion process of a Pt cluster, we observed a self-rotational motion (that is, a pivotal or wagging motion or both). Although a similar rotational motion of a cluster has been reported in other studies,[22,26] little research has been conducted on details of this motion. In general, the lateral movement of a cluster is described by the parameter D_{cm} because a cluster moves as a whole entity on the surface.[22] However, D_{cm} cannot properly describe the rotational motion of a cluster because the center of mass barely changes when the cluster rotates or wags itself on the z axis. To investigate the rotational properties of a cluster, we used the parameter D_{total}, which is the diffusion rate of all atoms in the cluster. Because D_{total} includes all atomic movements in the cluster, it can have several values during a rotational motion. Hence, the difference between D_{cm} and D_{total} can be a criterion for the rotational motion of a cluster. In this study, the rotation rate ($D_{rotation}$) of each cluster was evaluated by the formula, $100 \times (D_{total} - D_{cm})/D_{total}$, to normalize the calculated values.

Table 1 also summarizes the rotation rates with the Pt cluster size. The rotation rates, which seem unaffected by the cluster size or the overall structure of the Pt cluster, are generally high when the diffusion rates (D_{cm}) are low. They
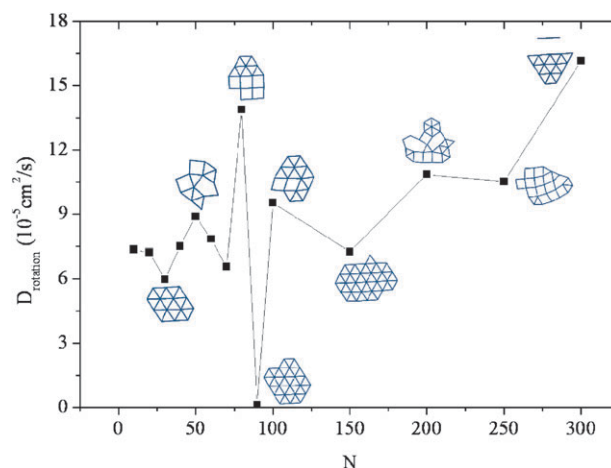

Fig. 3 Variation of rotation rates and bottom layers with cluster size.

include Pt_{50}, Pt_{60}, Pt_{80}, Pt_{100}, Pt_{200}, Pt_{250} and Pt_{300}. We can deduce therefore that rotation rates also depend significantly on the bottom layers of the Pt clusters just as the diffusion rates do. Fig. 3 shows the rotation rates and the bottom layers with the Pt cluster size. As shown in Fig. 2 and Fig. 3, the rotation rate has an inverse relation to the diffusion rate. These results can be explained by the difference in the diffusion rates of a hexagonal lattice and a rectangular lattice. As mentioned earlier, a cluster with a hexagonal lattice diffuses relatively faster due to lattice match with a graphite surface than a cluster with a rectangular lattice or a mixed one. A cluster that has two different types of lattices in the bottom layer has two different diffusion rates simultaneously. That is, one part of the bottom layer has a fast diffusion rate and the other part has a slow diffusion rate. Thus, because of the difference in the diffusion rates, the cluster rotates on a pivot, which is the slower diffusion part on the bottom layer. This phenomenon is clearly observable in the Pt_{80} cluster.

In addition to the rotation rate, we investigated the total movements of all atoms in the Pt_{80} cluster during the diffusion
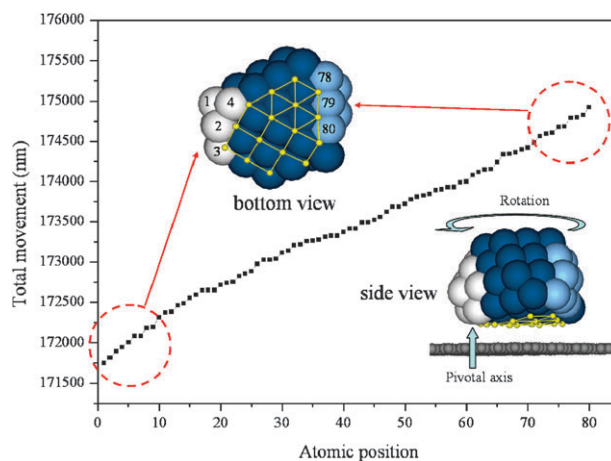

Fig. 4 Total movements of all atoms, with bottom and side views of the Pt_{80} cluster.

process. Fig. 4 shows the bottom and side views of the Pt_{80} cluster, revealing the total movements with each atom. In this figure, the difference in the total movements varies by as much as 3500 nm. Due to pivotal rotation, the total movements of each atom differ depending on the atomic position in the cluster even though all atoms are in the same cluster. The atoms with fewer movements (namely white atoms numbered 1 to 4) are mainly located on the rectangular lattice part of the cluster, whereas the atoms with a greater number of movements (namely gray atoms numbered 78 to 80) are located on the hexagonal part. As shown in the side view of Fig. 4, these results reveal that a Pt cluster rotates on the rectangular part of the cluster as a pivot during the diffusion process. The results also support our explanation of the rotational mechanism of a cluster: that is, the rotation of a cluster is caused by the difference in diffusion rates, which in turn depends on the various types of lattices in the bottom layer.

A Pt cluster that consists mainly of a hexagonal bottom layer sometimes tends to rotate well during the rapid diffusion because, as shown in the Pt_{150} cluster, the bottom layer is asymmetric. However, if the bottom layer consists mainly of a rectangular lattice, the cluster suffers from diffusion in all directions. The cluster consequently tends to rotate or wag itself on the z axis and not diffuse a long distance, as in the Pt_{200} and Pt_{250} clusters. This behavior is also explained well in terms of our diffusion mechanism.

On the basis of these results, we suggest that the cluster with a rectangular lattice is more effective than the cluster with a hexagonal lattice to prevent the aggregation of clusters. Using two same sized clusters (Pt_{192} with 16 atoms in the bottom layer) with different bottom layers, either a hexagonal lattice or a rectangular lattice, we observed that the cluster with a hexagonal lattice moves 1.7 times further than the cluster with rectangular lattice at the same running time (1 ns). This MD simulation clearly supports our suggestion.

Summary

In this study, we investigated the diffusion and rotation of Pt clusters supported on graphite. After the Pt clusters interact with graphite, they have two types of bottom layers: a hexagonal lattice and a rectangular lattice. The diffusion rates of Pt clusters are more dependent on the types of bottom layers than on any other factors. In the case of the hexagonal lattice, the Pt atoms in the bottom layer are periodically matched with stable sites on the graphite. This periodic matching enables a Pt cluster with a hexagonal lattice to diffuse faster and further than a cluster with a rectangular or a mixed lattice. Clusters that have a rectangular or mixed lattice tend to show pivotal rotation or wagging instead of lateral movement. For the mixed lattice, the difference in diffusion rates depending on the types of bottom layers causes the pivotal rotation of the Pt cluster. This rotational motion is clarified by the rotation rate and the total movements of all atoms in the Pt cluster. All of these results help us prevent undesirable aggregation of a supported cluster in practical application.

References

1 P. Jensen, *Rev. Mod. Phys.*, 1999, **71**, 1695.
2 V. Mehta and J. S. Cooper, *J. Power Sources*, 2003, **114**, 32–53.
3 S. H. Joo, S. J. Choi, I. Oh, J. Kwak, Z. Liu, O. Terasaki and R. Ryoo, *Nature*, 2001, **412**, 169–172.
4 A. C. C. Tseung and S. C. Dhara, *Electrochim. Acta*, 1975, **20**, 681–683.
5 E. Ganz, K. Sattler and J. Clarke, *Phys. Rev. Lett.*, 1988, **60**, 1856.
6 E. Ganz, K. Sattler and J. Clarke, *Surf. Sci.*, 1989, **219**, 33–67.
7 S. Eppell, G. S. Chottiner, D. A. Scherson and G. Pruett, *Langmuir*, 1990, **6**, 1316–1319.
8 F. Atamny and A. Baiker, *Surf. Interface Anal.*, 1999, **27**, 512–516.
9 S. Lee, H. Permana and K. Y. S. Ng, *J. Vac. Sci. Technol., B*, 1992, **10**, 561–565.
10 G. W. Clark and L. L. Kesmodel, *J. Vac. Sci. Technol., B*, 1993, **11**, 131–136.
11 S. H. Lee, H. Permana and K. Y. S. Ng, *Catal. Lett.*, 1994, **23**, 281–292.
12 I. Lee, K.-Y. Chan and D. L. Phillips, *Appl. Surf. Sci.*, 1998, **136**, 321–330.
13 I. Lee, K. Y. Chan and D. L. Phillips, *Ultramicroscopy*, 1998, **75**, 69–76.
14 P. Shen, N. Chi, K.-Y. Chan and D. L. Phillips, *Appl. Surf. Sci.*, 2001, **172**, 159–166.
15 N. Chi, K. Y. Chan and D. L. Phillips, *Catal. Lett.*, 2001, **71**, 21–26.
16 J. V. Zoval, J. Lee, S. Gorer and R. M. Penner, *J. Phys. Chem. B*, 1998, **102**, 1166–1175.
17 Y. Maruyama and J. Murakami, *Phys. Rev. B*, 2003, **67**, 085406.
18 L. Bardotti, P. Jensen, A. Hoareau, M. Treilleux and B. Cabaud, *Phys. Rev. Lett.*, 1995, **74**, 4694–4697.
19 L. Bardotti, P. Jensen, A. Hoareau, M. Treilleux, B. Cabaud, A. Perez and F. C. S. Aires, *Surf. Sci.*, 1996, **367**, 276–292.
20 E. J. Lamas and P. B. Balbuena, *J. Phys. Chem. B*, 2003, **107**, 11682–11689.
21 J. Chen and K. Y. Chan, *Mol. Simul.*, 2005, **31**, 527–533.
22 P. Deltour, J. L. Barrat and P. Jensen, *Phys. Rev. Lett.*, 1997, **78**, 4597–4600.
23 Z. H. Gu and P. B. Balbuena, *Catal. Today*, 2005, **105**, 152–161.
24 L. J. Lewis, P. Jensen, N. Combe and J. L. Barrat, *Phys. Rev. B*, 2000, **61**, 16084–16090.
25 S. Y. Liem and K. Y. Chan, *Surf. Sci.*, 1995, **328**, 119–128.
26 W. D. Luedtke and U. Landman, *Phys. Rev. Lett.*, 1999, **82**, 3835.
27 S. H. Lee, S. S. Han, J. K. Kang, J. H. Ryu and H. M. Lee, *Surf. Sci.*, 2008, **602**, 1433–1439.
28 G. Barcaro, A. Fortunelli, F. Nita and R. Ferrando, *Phys. Rev. Lett.*, 2005, **95**, 246103.
29 J. M. Wen, S. L. Chang, J. W. Burnett, J. W. Evans and P. A. Thiel, *Phys. Rev. Lett.*, 1994, **73**, 2591.
30 K. Morgenstern, G. Rosenfeld, B. Poelsema and G. Comsa, *Phys. Rev. Lett.*, 1995, **74**, 2058.
31 G. L. Kellogg, *Phys. Rev. Lett.*, 1994, **73**, 1833.
32 H. Brune, *Surf. Sci. Rep.*, 1998, **31**, 125.
33 T. Ala-Nissila, R. Ferrando and S. C. Ying, *Adv. Phys.*, 2002, **51**, 949.
34 Rifkin, the Center for Simulation, University of Connecticut, http://xmd.sourceforge.net.
35 T. Cagin, Y. Kimura, Y. Qi, H. Ikeda, W. L. Johnson and W. A. G. III, *Materials Research Society Symposia Proceedings*, Materials Research Society, Pittsburgh, 1999, vol. 554, p. 43.
36 S. P. Huang, D. S. Mainardi and P. B. Balbuena, *Surf. Sci.*, 2003, **545**, 163–179.
37 V. R. Bhethanabotla and W. A. Steele, *Phys. Rev. B*, 1990, **41**, 9480.
38 F. Baletto, R. Ferrando, A. Fortunelli, F. Montalenti and C. Mottet, *J. Chem. Phys.*, 2002, **116**, 3856.
39 S. P. Huang and P. B. Balbuena, *Mol. Phys.*, 2002, **100**, 2165–2174.